

Mathematical Modeling of Carbon Dioxide Removal from the CO₂/CH₄ Gas Mixture Using Amines and Blend of Amines in Polypropylene: A Comparison between Hollow Fiber Membrane Contactor and Other Membranes

Mohammad Reza Talaghat* and Ahmad Reza Bahmani

Department of Chemical Engineering, Petroleum and Gas, Shiraz University of Technology, Shiraz, Iran

ABSTRACT

In this work, a mathematical model is established to describe the removal of CO₂ from gaseous mixtures including CH₄ and CO₂ in a polypropylene hollow fiber membrane contactor in the presence of conventional absorbents such as monoethanolamine (MEA), methyldiethanolamine (MDEA), and a blend of them. Modeling was performed in axial and radial directions under the fully-wet condition for countercurrent gas-liquid flow arrangement. Both of axial and radial diffusions have been considered in three segments, including shell, membrane, and tube. To evaluate the model, the results of this model were compared with the experimental data and the results of COMSOL software and the results were in agreement with the experimental data and COMSOL outputs. In addition, the effect of various parameters on the removal percentage of carbon dioxide from gas mixtures was studied. It was found out that the CO₂ removal percentage is the best by using MEA solution as the absorbent. This modeling shows that the removal of CO₂ increases by adding MEA into MDEA solution. In this study, the factors that influence the removal percentage of CO₂ from gaseous mixture were investigated. The CO₂ removal efficiency increased with an increase in the liquid flow rate, number of fibers, membrane length, porosity-to-tortuosity ratio, and solvent concentration. The results show that increasing gas flow rate reduces CO₂ removal due to decreasing the contact time. Finally, the performance of this membrane was compared with other membranes such as polyvinyl difluoride (PVDF) and polytetrafluoroethylene (PTFE). The results show that the percentage of CO₂ removal by the polypropylene HFM is higher than that of the PVDF and PTFE hollow fiber membranes in the presence of MEA as the absorbent.

Keywords: Hollow Fiber Membrane, CO₂ Removal, Separation, Modeling, Blend of Amines.

INTRODUCTION

The emissions of greenhouse gases in the atmosphere are generally made by industries. In this regard, fossil fuel (coal, oil, and natural gas) burning is the main source of commercial energy supplies [1]. The flue

gases generally consist of nitrogen, oxygen, water vapor, carbon dioxide, sulfur dioxide, nitrogen oxides, and a small quantity of hydrochloric acid [2]. The major parts of the effluent gases are N₂, H₂O, and CO₂ [2,3]. Thus, an important step in

*Corresponding author

Mohammad Reza Talaghat
Email: talaghat@sutech.ac.ir
Tel: +98 71 3735 4520
Fax: +98 71 3735 4520

Article history

Received: May 02, 2016
Received in revised form: May 10, 2017
Accepted: June 18, 2017
Available online: November 15, 2017

many industrial processes is the removal of carbon dioxide from the process of gas streams because of technical and economical or environmental reasons. The conventional technology to capture CO₂ on a large scale is the absorption-desorption process. In this process, aqueous solutions such as monoethanolamine (MEA), diethanolamine (DEA), N-methyldiethanolamine (MDEA) are frequently used as absorbents [3]. In many chemical and petroleum refining processes, the gas absorption operation has been carried out using Venturi scrubbers, packed columns, and plate columns. These processes suffer a number of shortcomings such as flooding, channeling, entraining, foaming, and high capital and operating cost. In recent years, membrane-based technology is widely used in purification, concentration, and fractionation of fluid mixtures. In recent years, membrane gas absorption technology has been considered as one of the promising alternatives to conventional techniques for CO₂ capture due to its favorable mass transfer performance. As a hybrid approach of chemical absorption and membrane separation, it exhibits a number of advantages such as operational flexibility, compact structure, high surface-area-to-volume ratio, linear scale up, modularity, and predictable performance. A schematic drawing of membrane gas absorption process is shown in Figures 1 and 2.

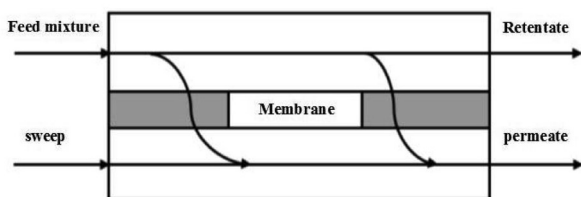


Figure 1: A general membrane process.

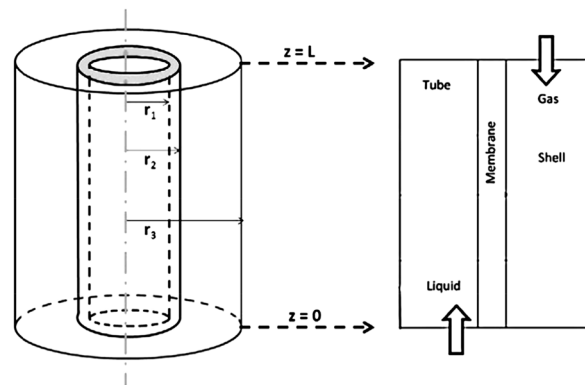


Figure 2: A schematic diagram of the hollow fiber membrane contactor.

The feed gas passes through the shell side of the hollow fibers, and the liquid absorbent flows countercurrent on the other side. Instead of depending on the membrane selectivity, the liquid flowing in the hollow fiber membrane contactor provides the selectivity and the porous, unselective membrane only acts as the contacting interface of the liquid and gas phases. The gasses diffuse through the membrane pores to the other side of the membrane where they are absorbed in the absorbent and taken away from the contactor. Although the membrane contactor offers many advantages over conventional contacting equipment, the resistance of additional mass transfer is introduced due to the existence of membrane phase. The membrane pores can be theoretically filled with either gas for the hydrophobic membrane or liquid for the hydrophilic membrane, corresponding to the non-wetting mode and overall-wetting mode respectively. For membrane gas absorption systems, it is essential to avoid a strong increase in mass transfer resistance in a liquid filled membrane pore compared to a gas-filled pore. However, in practical application, the aqueous solutions with organic absorbents can penetrate into partial pores of the hydrophobic membrane, and the membrane contactor is operated under partial wetting mode. The wetting phenomenon of

the membrane leads to an increase in the overall mass transfer resistance and the deterioration of membrane performance [4].

Polymeric membranes in the form of sheets or fine hollow fibers can be used to separate gas and liquid mixtures due to differences in permeation rates through the material. This makes membrane process very useful for a wide range of separations. One of the main challenges of membrane gas absorption technology is the membrane wetting by absorbent over prolonged operating time, which may significantly decrease the mass transfer coefficients of the membrane module. The characterization results from several types of research showed that the absorbent molecules diffused into the membrane polymer such as polypropylene during the contact with the membrane, resulting in the swelling of the membrane. In addition, the effects of operating parameters such as immersion time and absorbent type on the membrane wetting are important [5-9].

For the membrane gas absorption process, the membrane does not provide the selectivity. It only acts as the gas-liquid contact interface. Generally, hydrophobic porous membranes can be used as a gas-liquid membrane contactor. The most widely used hydrophobic polymers include PP, PVDF, PTFE, and PE membranes. PP, PTFE, and PE membranes are usually prepared by stretching and thermal methods, while PVDF asymmetric membranes are prepared via phase inversion method. PP and PE hollow fiber membranes are widely used in industries due to their low cost and commercial availability in various sizes, but their hydrophobicity is lower than membranes based on PTFE, PVDF, and other fluorine-containing polymers [4].

The absorption of carbon dioxide using the

chemical absorbent in microporous membrane was first studied by Qi and Cussler [10]. Karoor and Sirkar investigated the absorption of CO₂ and SO₂ in a microporous polypropylene hollow fibers using water as solvent [11]. Dindore et al. [12] investigated the chemical absorption of carbon dioxide using potassium carbonate in polypropylene hollow fiber membrane contactor. The absorption of CO₂ in different absorbents using the hollow fiber membrane contactors was reported by Wang et al. [13]. Al-Marzouqi et al. [14] developed a steady state mathematical model for micro porous hollow fiber membrane contactor to analyze the absorption of CO₂ using chemical absorbent.

In this study, the separation of CO₂ from CH₄ in a polypropylene hollow fiber membrane (HFM) is modeled in two dimensions using amine and a blend of amines. The model is based on fully wet conditions where the solvent completely filled the membrane pores. The effects of different parameters and membrane features on the percentage of CO₂ removal will be considered.

MATHEMATICAL MODELING

The mathematical modeling was performed in axial and radial directions to describe the removal of CO₂ from gaseous mixture in a hollow fiber membrane under the fully-wet condition in the presence of amine and a blend of amines. The model was based on the complete wetting condition in which the solvent completely filled the membrane pores. The schematic diagram for the hollow fiber membrane contactor is shown in Figure 2. The hollow fiber membrane contactor consists of three segments: tube side, membrane, and shell side. The liquid flows in the tube side, and the gas mixture flows in the shell side.

The following assumptions have been made in the mathematical model:

- 1) The hollow fiber membrane contactor is under steady state and isothermal conditions.
- 2) The Henry's law is applicable.
- 3) A complete wetting condition in which the solvent completely fills the membrane pores is considered.

Subject to these assumptions, the equation for absorption of CO₂ in the shell side of the hollow fiber membrane contactor in cylindrical coordinate is obtained using Fick's law:

$$D_{CO_2-shell} \left[\frac{\partial^2 C_{CO_2-shell}}{\partial r^2} + \frac{1}{r} \frac{\partial C_{CO_2-shell}}{\partial r} + \frac{\partial^2 C_{CO_2-shell}}{\partial z^2} \right] = \quad (1)$$

$$V_{z-shell} \frac{\partial C_{CO_2-shell}}{\partial z}$$

Radial velocity profile in the outside of hollow fiber is given by Equation 2 [15]:

$$V_{z-shell} = 2\bar{u}_{gas} \left[1 - \left(\frac{r_2}{r_3} \right)^2 \right] \left[\frac{\left(\frac{r}{r_3} \right)^2 - \left(\frac{r_2}{r_3} \right)^2 + 2 \ln \left(\frac{r_2}{r} \right)}{3 + \left(\frac{r_2}{r_3} \right)^4 - 4 \left(\frac{r_2}{r_3} \right)^2 + 4 \ln \left(\frac{r_2}{r_3} \right)^2} \right] \quad (2)$$

The boundary conditions are:

$$z = L \quad C_{CO_2-shell} = C_{CO_2-shell,initial} \quad (3)$$

$$r = r_2 \quad C_{CO_2-shell} = \frac{C_{CO_2-membrane}}{m} \quad (4)$$

$$r = r_3 \quad \frac{\partial C_{CO_2-shell}}{\partial r} = 0 \quad (5)$$

where, $D_{CO_2-shell}$ is the diffusion coefficient of CO₂ in shell (m².s⁻¹), and $C_{CO_2-shell}$ is the concentration of CO₂ in the shell (mol.m⁻³); $C_{CO_2-shell,initial}$ is the inlet CO₂ concentration in shell (mol.m⁻³), and $C_{CO_2-membrane}$ represents the concentration of CO₂ in the membrane (mol.m⁻³); $V_{z-shell}$ stands for the axial gas velocity in shell (m.s⁻¹); r_1 and r_2 represent the inner and outer

tube radius respectively, and r_3 is the inner shell radius (m); m is Henry's law constant, and L is the membrane length (m). The kinetic parameters for CO₂ and amines are given in Tables 1 to 6.

Within the membrane pore, the steady-state continuity equation for CO₂ is:

$$D_{CO_2-membrane} \left[\frac{\partial^2 C_{CO_2-membrane}}{\partial r^2} + \frac{1}{r} \frac{\partial C_{CO_2-membrane}}{\partial r} + \frac{\partial^2 C_{CO_2-membrane}}{\partial z^2} \right] + R_{CO_2} = 0 \quad (6)$$

$$D_{solvent-membrane} \left[\frac{\partial^2 C_{solvent-membrane}}{\partial r^2} + \frac{1}{r} \frac{\partial C_{solvent-membrane}}{\partial r} + \frac{\partial^2 C_{solvent-membrane}}{\partial z^2} \right] + R_{solvent} = 0 \quad (7)$$

The boundary conditions are given by the following equations:

$$r = r_2 \quad C_{CO_2-membrane} = m C_{CO_2-shell} \quad (8)$$

$$\frac{\partial C_{solvent-membrane}}{\partial r} = 0$$

$$r = r_1 \quad C_{CO_2-membrane} = C_{CO_2-tube} \quad (9)$$

$$C_{solvent-membrane} = C_{solvent-tube}$$

Within the tube side, the steady-state continuity equation for CO₂ and absorbent is defined by:

$$D_{CO_2-tube} \left[\frac{\partial^2 C_{CO_2-tube}}{\partial r^2} + \frac{1}{r} \frac{\partial C_{CO_2-tube}}{\partial r} + \frac{\partial^2 C_{CO_2-tube}}{\partial z^2} \right] + R_{CO_2} = 0 \quad (10)$$

$$= V_{z-tube} \frac{\partial C_{CO_2-tube}}{\partial z}$$

$$D_{\text{solvent-tube}} \left[\frac{\partial^2 C_{\text{solvent-tube}}}{\partial r^2} + \frac{1}{r} \frac{\partial C_{\text{solvent-tube}}}{\partial r} + \frac{\partial^2 C_{\text{solvent-tube}}}{\partial z^2} \right] + R_{\text{solvent}} \quad (11)$$

$$= V_{z\text{-tube}} \frac{\partial C_{\text{solvent-tube}}}{\partial z}$$

The radial velocity profile in the tube is assumed to follow the Newtonian laminar flow [16]:

$$V_{z\text{-tube}} = 2\bar{u}_{\text{liq}} \left[1 - \left(\frac{r}{r_1} \right)^2 \right] \quad (12)$$

The boundary conditions are given by the following equations:

$$z = 0 \quad C_{\text{CO}_2\text{-tube}} = 0 \quad (13)$$

$$C_{\text{solvent-tube}} = C_{\text{solvent-tube,initial}}$$

$$r = 0 \quad \frac{\partial C_{\text{CO}_2\text{-tube}}}{\partial r} = 0 \quad (14)$$

$$\frac{\partial C_{\text{solvent-tube}}}{\partial r} = 0$$

$$r = r_1 \quad C_{\text{CO}_2\text{-tube}} = C_{\text{CO}_2\text{-membrane}} \quad (15)$$

$$C_{\text{solvent-tube}} = C_{\text{solvent-membrane}}$$

Method of Solution

The set of partial differential equations along with boundary conditions and the reaction rates were solved

by numerical method using MATLAB software. In this study, we used finite difference method for the numerical solutions of differential equations. The physical and chemical properties are listed in Tables 1-6 [17].

RESULTS AND DISCUSSION

Today, the gas-liquid hollow fiber membrane contactors have been a subject of great interest. In these processes, the membrane contactor mainly acts as a physical barrier between two phases (gas and liquid) without any varieties in selectivity. Because of a very high surface/volume ratio, the hollow fiber membrane contactors have a great potential for gas absorption. In this work, mathematical model was performed in axial and radial directions for the removal of CO₂ in the hollow fiber membrane contactors in the presence of MEA, MDEA, and a blend of them under the fully-wet condition for a countercurrent gas-liquid flow arrangement. In this study, the effect of various parameters on the rate of the removal of carbon dioxide from gas mixtures were studied, and the results are presented in the following sections. The effect of gas flow rate on outlet CO₂ concentration in the membrane contractor is displayed in Figure 3.

Table 1: Diffusion coefficient of CO₂ and amine in tube and shell at T = 298 K [19-21].

MEA (B)+MDEA (C)+H ₂ O	
$k_{2,B} (\text{m}^3 \text{mol}^{-1} \text{s}^{-1})$	8.98
$\frac{k_{2,B} k_{\text{H}_2\text{O}}}{k_{-1}} (\text{m}^6 \text{mol}^{-2} \text{s}^{-1})$	1.16×10^{-5}
$\frac{k_{2,B} k_B}{k_{-1}} (\text{m}^6 \text{mol}^{-2} \text{s}^{-1})$	2.41×10^{-3}
$\frac{k_{2,B} k_C}{k_{-1}} (\text{m}^6 \text{mol}^{-2} \text{s}^{-1})$	5.31×10^{-4}
$k_{2,C} (\text{m}^3 \text{mol}^{-1} \text{s}^{-1})$	1.30×10^{-3}

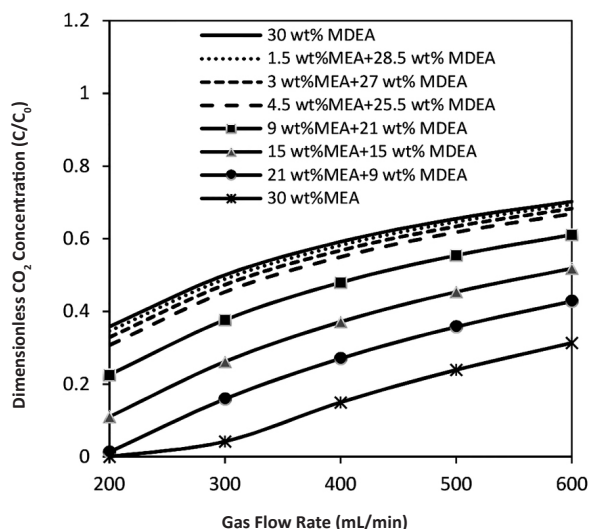


Figure 3: The effect of gas flow rate on outlet CO₂ concentration in the membrane contactor for the absorption of CO₂ ($n = 3600$, $Q_{\text{Liquid}} = 500$ mL/min, $C_{o, \text{gas}} = 3.883$ mol/m³, $L = 0.2286$ m, $\epsilon/\tau = 0.2$, $T = 313$ K).

Table 2: Parameters used in simulation at T=313 K [19-21].

Parameter	Value	Ref.
Inner tube radius(mm)(R_1)	0.11	[21]
Outer tube radius (mm) (R_2)	0.15	[21]
Inner shell radius (mm) (R_3)	0.2645	[21]

Table 3: Kinetic parameters for the blend of amines at T=313 K in tube and shell [19].

Tube Section	
$D_{\text{MEA-tube}}$ (30 wt.% MEA)	8.590×10^{-10}
$D_{\text{MEA-tube}}$ (21 wt.% MEA+9 wt.% MDEA)	8.356×10^{-10}
$D_{\text{MEA-tube}}$ (15 wt.% MEA+15 wt.% MDEA)	8.181×10^{-10}
$D_{\text{MEA-tube}}$ (9 wt.% MEA+21 wt.% MDEA)	7.985×10^{-10}
$D_{\text{MEA-tube}}$ (4.5 wt.% MEA+25.5 wt.% MDEA)	7.821×10^{-10}
$D_{\text{MEA-tube}}$ (3 wt.% MEA+27 wt.% MDEA)	7.769×10^{-10}
$D_{\text{MEA-tube}}$ (1.5 wt.% MEA+28.5 wt.% MDEA)	7.705×10^{-10}
$D_{\text{MDEA-tube}}$ (30 wt.% MDEA)	7.642×10^{-10}
$D_{\text{MDEA-tube}}$ (21 wt.% MEA+9 wt.% MDEA)	5.584×10^{-10}
$D_{\text{MDEA-tube}}$ (15 wt.% MEA+15 wt.% MDEA)	5.565×10^{-10}
$D_{\text{MDEA-tube}}$ (9 wt.% MEA+21 wt.% MDEA)	5.332×10^{-10}
$D_{\text{MDEA-tube}}$ (4.5 wt.% MEA+25.5 wt.% MDEA)	5.221×10^{-10}
$D_{\text{MDEA-tube}}$ (3 wt.% MEA+27 wt.% MDEA)	5.181×10^{-10}
$D_{\text{MDEA-tube}}$ (1.5 wt.% MEA+28.5 wt.% MDEA)	5.141×10^{-10}
$D_{\text{CO}_2\text{-tube}}$ (30 wt.% MEA)	11.509×10^{-9}
$D_{\text{CO}_2\text{-tube}}$ (21 wt.% MEA+9 wt.% MDEA)	6.922×10^{-9}
$D_{\text{CO}_2\text{-tube}}$ (15 wt.% MEA+15 wt.% MDEA)	4.484×10^{-9}
$D_{\text{CO}_2\text{-tube}}$ (9 wt.% MEA+21 wt.% MDEA)	3.102×10^{-9}
$D_{\text{CO}_2\text{-tube}}$ (4.5 wt.% MEA+25.5 wt.% MDEA)	2.346×10^{-9}
$D_{\text{CO}_2\text{-tube}}$ (3 wt.% MEA+27 wt.% MDEA)	2.760×10^{-9}
$D_{\text{CO}_2\text{-tube}}$ (1.5 wt.% MEA+28.5 wt.% MDEA)	2.047×10^{-9}
$D_{\text{CO}_2\text{-tube}}$ (30 wt.% MDEA)	1.960×10^{-9}
Shell Section	
$D_{\text{CO}_2\text{-shell}}$ (CH ₄ /CO ₂)	1.9968×10^{-5}
$D_{\text{CO}_2\text{-shell}}$ (N ₂ /CO ₂)	1.2498×10^{-5}

Table 4: The diffusion coefficient of CO₂ and amines.

Tube Section	
D _{AMP-tube}	1.18×10 ⁻⁹
D _{MEA-tube}	1.51×10 ⁻⁹
D _{DEA-tube}	1.47×10 ⁻⁹
D _{MDEA-tube}	1.44×10 ⁻⁹
D _{CO₂ tube} (aqueous AMP solution)	5.67×10 ⁻¹⁰
D _{CO₂ tube} (aqueous MEA solution)	9.32×10 ⁻¹⁰
D _{CO₂ tube} (aqueous DEA solution)	6.32×10 ⁻¹⁰
D _{CO₂ tube} (aqueous MDEA solution)	6.21×10 ⁻¹⁰
Shell Section	
D _{CO₂ shell} (CH ₄ /CO ₂)	1.18×10 ⁻⁵
D _{CO₂ shell} (N ₂ /CO ₂)	1.18×10 ⁻⁵

Table 5: Rate expression of amines.

Aqueous amine solution	R _B (mol.m ⁻³ s ⁻¹)	R _C (mol.m ⁻³ .s ⁻¹)	Reference
Single amines MEA (B): MDEA (B):	$\frac{K_{2,B}C_{CO_2}C_B}{1 + \left(\left(\frac{K_{H_2O}}{K-1} \right) C_{H_2O} \right) + \left(\left(\frac{K_B}{K-1} \right) C_B \right)}$ $k_{2,B}C_{CO_2}C_B$		[21]
Blended amines MEA (B) +MDEA (C)	$\frac{K_{2,B}C_{CO_2}C_B}{1 + \left(\left(\frac{K_{H_2O}}{K-1} \right) C_{H_2O} \right) + \left(\left(\frac{K_B}{K-1} \right) C_B \right) + \left(\left(\frac{K_C}{K-1} \right) C_C \right)}$	$k_{2,C}C_{CO_2}C_C$	

Table 6: Kinetic parameters for pure of amine at T=298 K [17, 18, 19]

$k_{2,B}(\text{m}^3\text{mol}^{-1}\text{s}^{-1})$	$\frac{k_{2,B}k_{H_2O}}{k_{-1}}(\text{m}^6\text{mol}^{-2}\text{s}^{-1})$	$\frac{k_{2,B}k_B}{k_{-1}}(\text{m}^6\text{mol}^{-2}\text{s}^{-1})$
MEA (B)+H ₂ O		
6.358	$9.58 \cdot 10^{-6}$	$1.58 \cdot 10^{-3}$
MDEA (B)+H ₂ O		
$5.21 \cdot 10^{-3}$		

This figure shows that the outlet CO₂ concentration in the shell side increases with increasing gas flow rate. This is due to a decrease in the residence time of CO₂ in shell, which in turn reduces the removal percentage of CO₂ along the length of the module and further the reduction of CO₂ availability for the reactive absorption. The dimensionless CO₂

concentration along the length of the module for the different compositions of a blend of amines is presented in Figure 4. To evaluate the model, the results of this model were compared with the experimental data from references [17-18] and the results of COMSOL software. This comparison is illustrated in Figure 5.

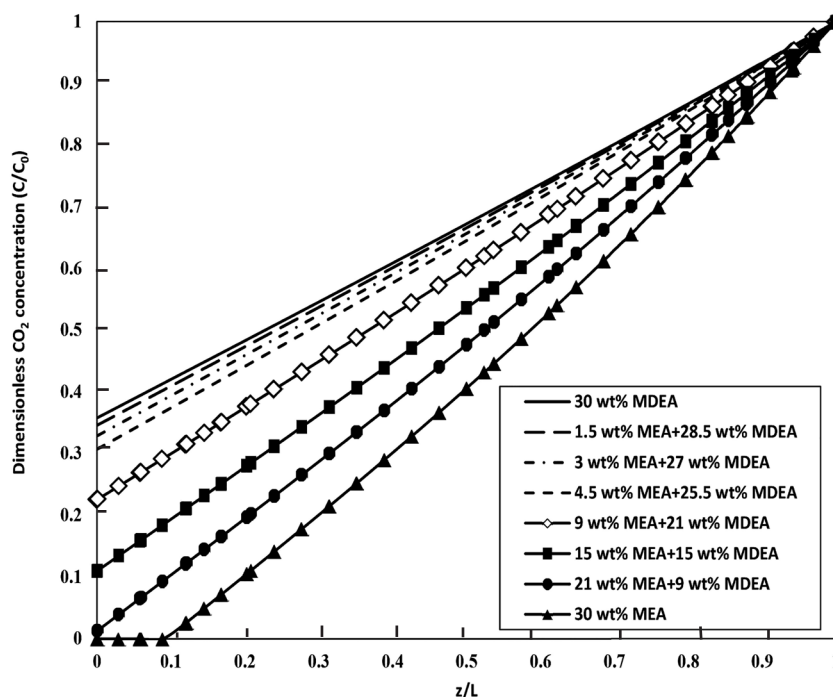


Figure 4: CO₂ concentration in the axial direction at different compositions of mixed amines; ($n=3600$, $Q_{GAS}=500$ mL/min, $Q_{LIQUID}=500$ mL/min, $C_{O,GAS}=3.883$ mol/m³, $L=0.2286$ m, $\epsilon/\tau=0.2$, $T=313$ K).

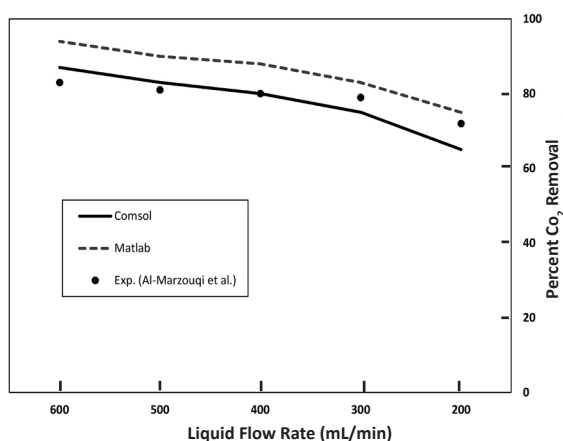


Figure 5: Comparison of results from this modeling with experimental data and COMSOL software results for MEA solution; $n = 3600$, $Q_{Gas} = 500$ mL/min, $C_{o, Gas} = 3.883$ mol/m³, $C_{CO_2-initial} = 4$ mol/m³, $L = 0.2286$ m, $\epsilon/\tau = 0.2$, $T = 298$ K

The results show good agreement. The outlet CO₂ concentration at different liquid flow rates in the shell side is illustrated in Figure 6.

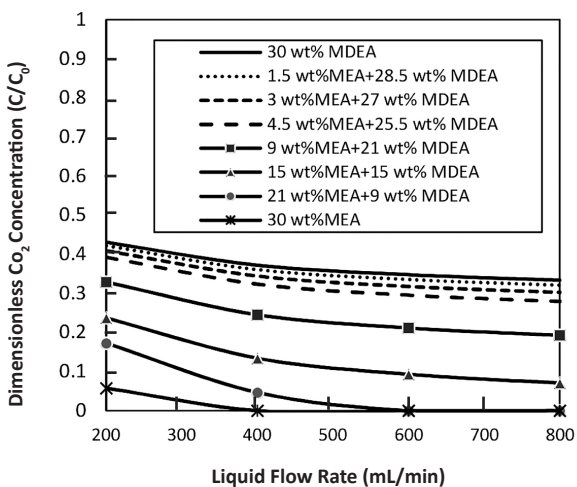


Figure 6: The effect of liquid flow rate on outlet CO₂ concentration in the membrane contactor for the absorption of CO₂; ($n = 3600$, $Q_{Gas} = 200$ mL/min, $C_{o, Gas} = 3.883$ mol/m³, $L = 0.2286$ m, $\epsilon/\tau = 0.2$, $T = 313$ K).

As can be seen from this figure, the outlet CO₂ concentration drops with an increase in the liquid flow rate. This is due to an increase in the concentration gradients of CO₂ in the liquid phase; thus, the outlet CO₂ concentration in gas becomes less and the CO₂ removal percentage increases. As the absorbent

moves faster, the CO₂ outlet concentration in gas phase rises, and the CO₂ removal rate augments. The outlet CO₂ concentration in the shell decreases with increasing the total number of fibers due to an increase in the interface of mass transfer contact. These results are presented in Figure 7. This figure shows that increasing the number of fibers in membrane modules will encourage the CO₂ removal percentage in the membrane contactor for the absorption of CO₂.

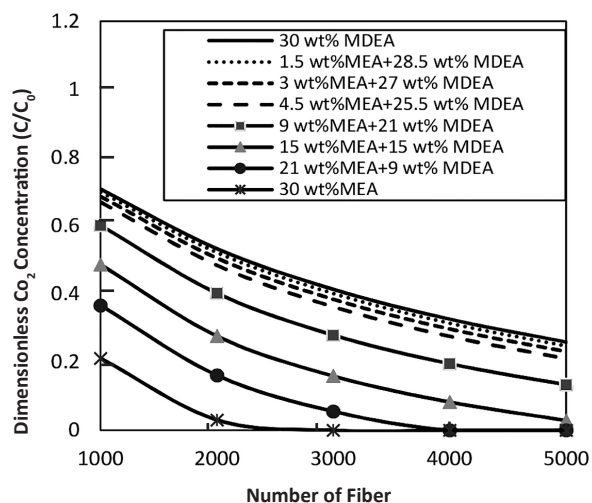


Figure 7: The effect of the number of fibers on outlet CO₂ concentration in the membrane contactor for the absorption of CO₂. ($Q_{Liquid} = 500$ mL/min, $Q_{Gas} = 200$ mL/min, $C_{o, Gas} = 3.883$ mol/m³, $L = 0.2286$ m, $\epsilon/\tau = 0.2$, $T = 313$ K).

The effect of porosity-to-tortuosity ratio of the outlet CO₂ concentration is shown in Figure 8. As the porosity-to-tortuosity ratio increases, the outlet CO₂ concentration decreases because the diffusion coefficient of CO₂ in the membrane is a function of membrane porosity and tortuosity. By increasing the porosity-to-tortuosity ratio, the membrane mass transfer resistance decreases. Therefore, the total resistance to the mass transfer of CO₂ drops.

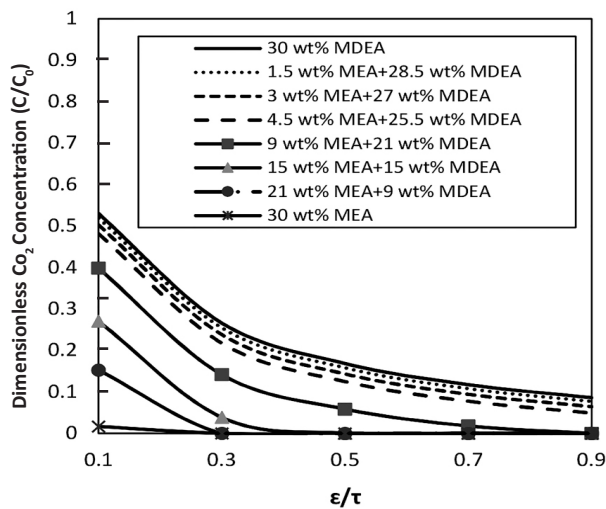


Figure 8: The effect of porosity-to-tortuosity ratio on outlet CO₂ concentration in the membrane contactor for the absorption of CO₂; ($n = 3600$, $Q_{\text{Liquid}} = 500 \text{ mL/min}$, $Q_{\text{Gas}} = 200 \text{ mL/min}$, $C_{\text{o, Gas}} = 3.883 \text{ mol/m}^3$, $L = 0.2286 \text{ m}$, $T = 313 \text{ K}$).

According to Equation 16, with increasing porosity-to-tortuosity ratio, which is provided by membrane manufacturer, the effective diffusion coefficient of CO₂ in the membrane increases.

$$D_{\text{CO}_2\text{-membrane}} = D_{\text{CO}_2\text{-tube}} \left(\frac{\varepsilon}{\tau} \right) \quad (16)$$

The outlet CO₂ concentration at different membrane lengths is demonstrated in Figure 9.

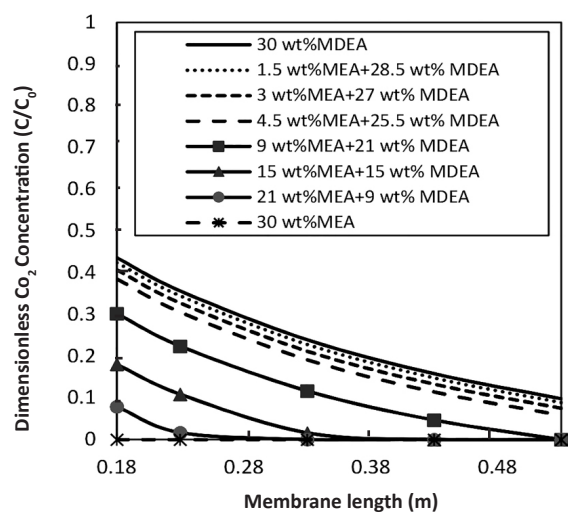


Figure 9: The effect of membrane length on outlet CO₂ concentration in the membrane contactor for the absorption of CO₂ ($n = 3600$, $Q_{\text{Liquid}} = 500 \text{ mL/min}$, $Q_{\text{Gas}} = 200 \text{ mL/min}$, $C_{\text{o, Gas}} = 3.883 \text{ mol/m}^3$, $\varepsilon/\tau = 0.2$, $T = 313 \text{ K}$).

As can be seen from this figure, the outlet CO₂ concentration decreases with increasing membrane length, which is because of an increase in the contact time of gas phase and liquid phase due to a longer membrane length. Furthermore, in this research the removal of CO₂ from gas mixture was modeled using a blend of amines. The results of modeling are shown in Figures 3 to 9. It can be inferred from these figures that the removal of CO₂ increases by increasing MEA concentration in the blend of MEA and MDEA. This is due to the fact that the absorption reaction rate of CO₂ in the presence of an MEA solution is much higher than that of CO₂ in the presence of an MDEA solution.

Also, the effect of liquid flow rate on the CO₂ removal percentage for various hollow fiber membranes such as PP, PVDF, and PTFE in the presence of MEA as the absorbent was studied; the results are shown in Figure 10.

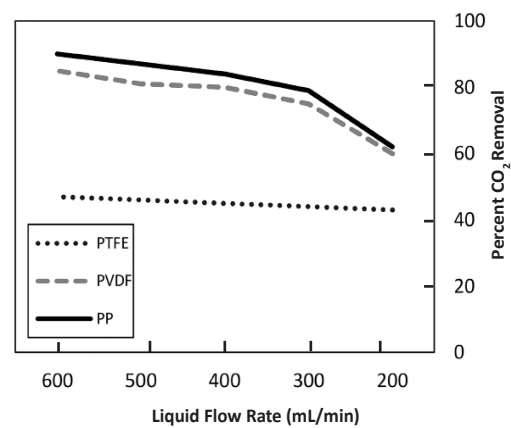


Figure 10: Effect of liquid flow rate on the CO₂ removal percentage for various hollow fiber membranes; ($C_{\text{MEA-initial}} = 10 \text{ mol/m}^3$, $C_{\text{CO}_2\text{-initial}} = 4 \text{ mol/m}^3$, $Q_{\text{Gas}} = 500 \text{ mL/min}$).

The results show that the percentage of CO₂ removal of the polypropylene hollow fiber membrane is higher than that of the PVDF and PTFE hollow fiber membranes. Finally, the outlet CO₂ concentration at different solvent concentrations is demonstrated in Figure 11. This figure shows that by increasing the concentrations of the solvent, the outlet concentration of carbon dioxide drops.

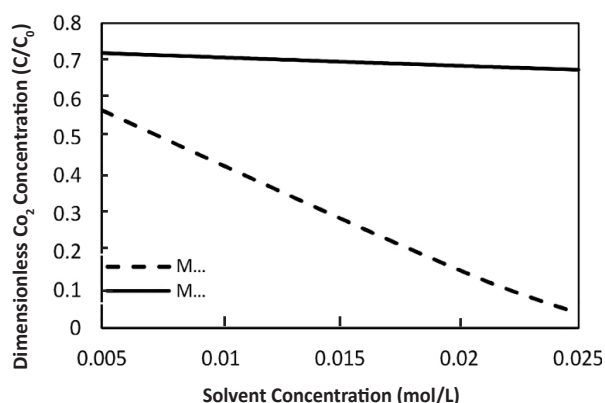


Figure 11: The effect of solvent concentration on the concentration of the outlet CO₂.

CONCLUSIONS

In this work, mathematical modeling was performed in axial and radial directions for the removal of CO₂ in the hollow fiber membrane contactors in the presence of MEA, MDEA, and a blend of them in a fully-wet condition for a countercurrent gas–liquid flow arrangement. Both of axial and radial diffusions have been considered in three segments of shell, membrane, and tube. The effects of liquid flow rate, gas flow rate, membrane length, porosity-to-tortuosity ratio, and total number of fibers were studied. The results of modeling indicated that the pure aqueous solution of MEA is the most suitable absorbent for the absorption of CO₂ among a mixture of MEA and MDEA solution. This modeling showed that the removal of CO₂ increases by adding MEA into MDEA aqueous solution. The reason is that the absorption reaction rate of CO₂ in the presence of an MEA solution is much higher than that of CO₂ in the presence of an MDEA solution. Also, the results of modeling showed that the removal of CO₂ is increased by decreasing gas flow rate, by increasing liquid flow rate, by extending membrane length, by increasing porosity-to-tortuosity ratio, and by raising the total number of fibers in the membrane

contactor. The experimental data agreed well with the mathematical model developed in this work. Furthermore, the results show that the percentage of CO₂ removal by the polypropylene hollow fiber membrane is higher than that of the PVDF and PTFE hollow fiber membranes in the presence of MEA as the absorbent.

Moreover, the following results of this study can be used for future works:

- 1- The selection type of amine and type of hollow fiber membrane for carbon dioxide separation;
- 2- The determination of gas and liquid flow rate range for carbon dioxide separation process in hollow fiber membranes.

Furthermore, the following items can be studied for further research in the future:

- 1- Ionic liquids can be used instead of the amines;
- 2- A comparison can be drawn between the physical and chemical solvents;
- 3- A comparison can be made between the co-current and counter-current operations;
- 4- The separation percentage of CO₂ in a hollow fiber membrane contactor and in the absorption tower with amines may be compared;
- 5- Removing carbon dioxide and hydrogen sulfide simultaneously can be studied.

ACKNOWLEDGEMENTS

The authors are grateful to the Shiraz University of Technology for supporting this work.

NOMENCLATURES

$C_{\text{CO}_2\text{-tube}}$: Concentration of CO ₂ in the tube (mol.m ⁻³)
$C_{\text{CO}_2\text{-membrane}}$: Concentration of CO ₂ in the membrane (mol.m ⁻³)
$C_{\text{CO}_2\text{-shell}}$: Concentration of CO ₂ in the shell (mol.m ⁻³)

$C_{\text{solvent-tube}}$: Concentration of solvent in the tube (mol.m^{-3})
$C_{\text{solvent-membrane}}$: Diffusion coefficient of CO_2 in membrane ($\text{m}^2.\text{s}^{-1}$)
$C_{\text{CO}_2\text{-shell,initial}}$: Diffusion coefficient of CO_2 in shell ($\text{m}^2.\text{s}^{-1}$)
$D_{\text{CO}_2\text{-tube}}$: Diffusion coefficient of CO_2 in tube ($\text{m}^2.\text{s}^{-1}$)
$D_{\text{CO}_2\text{-membrane}}$: Diffusion coefficient of CO_2 in membrane ($\text{m}^2.\text{s}^{-1}$)
$D_{\text{CO}_2\text{-shell}}$: Diffusion coefficient of CO_2 in shell ($\text{m}^2.\text{s}^{-1}$)
$D_{\text{solvent-tube}}$: Diffusion coefficient of solvent in tube ($\text{m}^2.\text{s}^{-1}$)
$D_{\text{solvent-membrane}}$: Diffusion coefficient of solvent in membrane ($\text{m}^2.\text{s}^{-1}$)
\bar{u}	: Average velocity (m.s^{-1})
ϵ	: Porosity (-)
L	: Length of fiber (m)
M	: Physical solubility (-)
n	: Total number of fibers (-)
Q_{gas}	: Gas flow rate (L.min^{-1})
Q_{liq}	: Liquid flow rate (L.min^{-1})
r_1	: inner tube radius (m)
r_2	: Outer tube radius (m)
r_3	: inner shell radius (m)
R_{CO_2}	: Overall reaction rate of CO_2 (mol.s^{-1})
R_{solvent}	: Overall reaction rate of solvent (mol.s^{-1})
$V_{z\text{-shell}}$: Velocity in shell (m.s^{-1})
$V_{z\text{-tube}}$: Velocity in tube (m.s^{-1})
τ	: Tortuosity (-)
Subscripts and Superscripts	
1	: inner tube
2	: outer tube
3	: inner shell

REFERENCES

- Zhang J., Webley P. A. and Xiao P., "Effect of Process Parameters on Power Requirements of Vacuum Swing Adsorption Technology for CO_2 Capture from Flue Gas," *Energy Conversion and Management*, **2008**, 49(2), 346-350.
- Powell C. E. and Qiao G. G., "Polymeric CO_2/N_2 Gas Separation Membranes for the Capture of Carbon Dioxide from Power Plant Flue Gases," *J. Membr. Sci.*, **2006**, 279, 1-10.
- Kohl A. L. and Nielsen R., "Gas Purification," Houston Texas: Gulf Publishing Company, **1997**.
- Wang R., Zhang H. Y., Feron P. H. M., and Liang D. T., "Influence of membrane wetting on CO_2 capture in microporous hollow fiber membrane contactors," *Separation and Purification Technology*, **2005**, 46, 33-40.
- Singh P. and Versteeg G. F., "Structure and Activity Relationships for CO_2 Regeneration from Aqueous Amine-based Absorbents," *Process Safety and Environmental Protection*, **2008**, 86, 347-359.
- Mavroudi M., Kaldis S. P., and Sakellariopoulos G. P., "A Study of Mass Transfer Resistance in Membrane Gas-liquid Contacting Process," *Journal of Membrane Science*, **2006**, 272, 103-115.
- Wang R., Li D. F., Zhou C., Liu M., and et al., "Impact of DEA Solutions with and without CO_2 Loading on Porous Polypropylene Membranes intended for Use as Contactors," *Journal of Membrane Science*, **2004**, 229, 147-157.
- Lv Y. X., Yu X. H., Tu S. T., Yan, J.Y., and et al., "Wetting of Polypropylene Hollow Fiber Membrane Contactors," *Journal of Membrane Science*, **2010**, 362, 444-452.
- Lv Y. X., Yu X. H., Tu S. T., Yan J. Y., and et al., "Experimental Studies on Simultaneous Removal of CO_2 and SO_2 in a Polypropylene Hollow Fiber Membrane Contactor," *International Conference on Applied Energy*, ICAE 2011, Italy, **2011**.
- Qi Z. and Cussler E. L., "Microporous Hollow Fibers for Gas Absorption," *J. Membr. Sci.*, **1985**, 23(3), 321-330.

11. Karoor S., and Sirkar K. K., "Gas Absorption Studies in Microporous Hollow Fiber Membrane Contactors," *J. Member Sci.*, **2001**, 194(4), 57-64.
12. Dindore V. Y., Brillman D. W. F., and Versteeg G. F., "Modeling of Cross-flow Membrane Contactors: Mass Transfer with Chemical Reactions," *J. Member Sci.*, **2005**, 255, 275-285.
13. Wang R., Li D., and Liang D., "Modeling of CO₂ Capture by Three Typical Amine Solution in Hollow Fiber Membrane Contactors," *Chem. Eng. Proc.*, **2004**, 43, 849-860.
14. Al-Marzougi M., El-Nass M., Marzouk S., Abdulkarimi M., and et al., "Modeling of CO₂ absorption in membrane contactors," *Sep. Purification Technology*, **2008**, 59(1), 286-292.
15. Happel J., "Viscous Flow Relative to Arrays of Cylinders," *AIChE J.*, **1959**, 5(1), 174-182.
16. Bird R. B., Stewart W. E., and Lightfoot E. N., "Transport Phenomena," New York: Wiley, **1960**.
17. Paul S., Ghoshal A. K., and Mandal B., "Removal of CO₂ by single and Blended Aqueous Alkanol amine Solvents in Hollow-Fiber Membrane Contactor: Modeling and Simulation," *Ind. Eng. Chem. Res.*, **2007**, 46, 2576-2585.
18. Al-Marzougi M., El-Nass M., Marzouk S., and Abdullatif N., "Modeling Chemical Absorption of CO₂ in Membrane Contactors," *Sep. Purifi. Technol.*, **2008**, 62, 499-515.
19. Versteeg G. F. and Van Swaalj W., "Solubility and Diffusivity of Acid Gases (Carbon Dioxide, nitrous Oxide) in Aqueous Alkanol Amine Solutions," *Journal of Chemical and Engineering Data*, **1988**, 33, 29-34.
20. Cussler E., "Diffusion: Mass Transfer in Fluid Systems, 1," *Cambridge University Press, Cambridge, Chapters*, **1984**, 1, 9-21.
21. Hagewiesche D. P., Ashour S. S., Al-Ghawas H. A., *Journal of Petroleum Science and Technology* **2017**, 7(4), 41-53